

# Proton-nucleus total reaction cross sections in the optical limit Glauber theory: Subtle dependence on the equation of state of nuclear matter

K. Iida,<sup>1,2</sup> K. Oyamatsu,<sup>2,3</sup> B. Abu-Ibrahim,<sup>2,4</sup> and A. Kohama<sup>2</sup>

<sup>1</sup>*Department of Natural Science, Kochi University, Akebono-cho, Kochi 780-8520, Japan*

<sup>2</sup>*RIKEN Nishina Center, RIKEN, Wako-shi, Saitama 351-0198, Japan*

<sup>3</sup>*Department of Human Informatics, Aichi Shukutoku University,*

*Nagakute, Nagakute-cho, Aichi-gun, Aichi 480-1197, Japan*

<sup>4</sup>*Department of Physics, Cairo University, Giza 12613, Egypt*

We calculate the proton-nucleus total reaction cross sections at different energies of incident protons within the optical limit approximation of the Glauber theory. The isospin effect has been taken into account. The nucleon distribution is obtained in the framework of macroscopic nuclear models in a way depending on the equation of state of uniform nuclear matter near the saturation density. We find that at an energy of order 40 MeV, the reaction cross section calculated for neutron-rich isotopes significantly increases as the parameter  $L$  characterizing the density dependence of the symmetry energy increases, while at energies of order 300 and 800 MeV, it is almost independent of  $L$ . This is a feature of the optical limit Glauber theory in which an exponential dependence of the reaction cross section on the neutron skin thickness remains when the total proton-neutron cross section is small enough.

PACS numbers: 25.60.Dz, 21.10.Gv, 25.60.-t, 24.10.Ht

Keywords:

## I. INTRODUCTION

Reactions of unstable neutron-rich nuclei with a proton target are of current interest as such reactions can act as a major means to probe the matter densities of exotic nuclei. If one appropriately selects incident energies, protons could be more sensitive to neutron distributions than to proton distributions of nuclei. The equation of state (EOS) of nuclear matter is also of interest since it is essential to understand the saturation property of atomic nuclei, the structure of neutron stars, and the mechanism of stellar collapse. In a previous work [1] we have theoretically connected the EOS of nuclear matter to the proton-nucleus elastic differential cross sections. We limited ourselves to high energy of order 800 MeV and used the optical limit approximation (OLA) of the Glauber theory. We find, at large neutron excess, a strong correlation between the peak angle in the small momentum transfer regime and the density symmetry coefficient  $L$ , which characterizes the density dependence of the symmetry energy and hence controls the size of neutron-rich nuclei [2]. At this high energy, we briefly addressed the question of how the total reaction cross sections and the EOS parameters connect and did not find a strong correlation as compared with the case of elastic scattering.

The purpose of the present paper is to study the connection between the EOS of nuclear matter and the proton-nucleus total reaction cross section in more detail and at different energies within the OLA of the Glauber theory. We are interested in the total reaction cross section because, for neutron-rich isotopes, it is much easier to measure experimentally than the elastic differential cross section and uncertainties in the measured reaction cross section are expected to be sufficiently small to deduce new information about the EOS parameters.

In the course of this study, however, we happened to find some interesting properties of the calculated total reaction cross sections, of which the physical manifestation remains to be examined. We will thus focus on these properties from a purely theoretical point of view, instead of deducing the EOS parameters from empirical data for the total reaction cross sections.

In Sec. II, we summarize a macroscopic nuclear model that allows us to connect the nucleon density distributions and the EOS of nuclear matter. Section III is devoted to description of the reaction cross sections within the framework of the Glauber theory. In Sec. IV, we calculate the reaction cross sections for heavy neutron-rich nuclei in a way dependent on the EOS of nuclear matter, which in turn are analyzed by using the rectangular distributions that allow for neutron skin thickness.

## II. FROM EQUATION OF STATE TO NUCLEI

In this section, we summarize the way we connect the nucleon density distributions with the EOS of nuclear matter. Generally, the energy per nucleon of nuclear matter can be expanded around the saturation point of symmetric nuclear matter as

$$w = w_0 + \frac{K_0}{18n_0^2}(n - n_0)^2 + \left[ S_0 + \frac{L}{3n_0}(n - n_0) \right] \alpha^2. \quad (1)$$

Here  $w_0$ ,  $n_0$ , and  $K_0$  are the saturation energy, the saturation density and the incompressibility of symmetric nuclear matter,  $n$  is the nucleon density, and  $\alpha$  is the neutron excess. The parameters  $L$  and  $S_0$  characterize the density dependent symmetry energy coefficient  $S(n)$ :  $S_0$  is the symmetry energy coefficient at  $n = n_0$ , and  $L = 3n_0(dS/dn)_{n=n_0}$  is the density symmetry coefficient.

As shown in Ref. [2] by describing macroscopic nuclear properties in a manner that is dependent on these EOS parameters, empirical data for masses and radii of stable nuclei can provide a strong constraint on the parameters  $w_0$ ,  $n_0$ , and  $S_0$ , while leaving  $K_0$  and  $L$  uncertain. We remark that the isoscalar giant monopole resonance in nuclei (e.g., Ref. [3]) and caloric curves in nuclear collisions (e.g., Ref. [4]) can constrain  $K_0$  only in a way that is dependent on models for the effective nucleon-nucleon interaction.

The incompressibility  $K_0$  and the density symmetry coefficient  $L$  control in which direction the saturation point moves on the density versus energy plane, as the neutron excess increases from zero. This feature can be found from the fact that up to second order in  $\alpha$ , the saturation energy  $w_s$  and density  $n_s$  are given by

$$w_s = w_0 + S_0\alpha^2 \quad (2)$$

and

$$n_s = n_0 - \frac{3n_0L}{K_0}\alpha^2. \quad (3)$$

The influence of  $K_0$  and  $L$  on neutron star structure can be significant [5] despite the fact that these parameters characterize the EOS near normal nuclear density and proton fraction, which are fairly low and large, respectively, as compared with the typical densities and proton fractions in the central region of the star.

We proceed to macroscopic nuclear models used in this and previous works [1, 2, 6]. We describe a spherical nucleus of proton number  $Z$  and mass number  $A$  within the framework of a simplified version of the extended Thomas-Fermi theory [7]. We first write the total energy of a nucleus as a function of the neutron and proton density distributions  $n_n(\mathbf{r})$  and  $n_p(\mathbf{r})$  in the form

$$E = E_b + E_g + E_C + (A - Z)m_n c^2 + Zm_p c^2, \quad (4)$$

where

$$E_b = \int d\mathbf{r} n(\mathbf{r}) w(n_n(\mathbf{r}), n_p(\mathbf{r})) \quad (5)$$

is the bulk energy with the energy per nucleon  $w(n_n, n_p)$  of uniform nuclear matter,

$$E_g = F_0 \int d\mathbf{r} |\nabla n(\mathbf{r})|^2 \quad (6)$$

is the gradient energy with adjustable constant  $F_0$ ,

$$E_C = \frac{e^2}{2} \int d\mathbf{r} \int d\mathbf{r}' \frac{n_p(\mathbf{r})n_p(\mathbf{r}')}{|\mathbf{r} - \mathbf{r}'|} \quad (7)$$

is the Coulomb energy, and  $m_n$  and  $m_p$  are the neutron and proton rest masses. We express  $w$  as [7]

$$w = \frac{3\hbar^2(3\pi^2)^{2/3}}{10m_n n} (n_n^{5/3} + n_p^{5/3}) + (1 - \alpha^2) \frac{v_s(n)}{n} + \alpha^2 \frac{v_n(n)}{n}, \quad (8)$$

where

$$v_s = a_1 n^2 + \frac{a_2 n^3}{1 + a_3 n} \quad (9)$$

and

$$v_n = b_1 n^2 + \frac{b_2 n^3}{1 + b_3 n} \quad (10)$$

are the potential energy densities for symmetric nuclear matter and pure neutron matter. This expression for  $w$  is one of the simplest parametrization that reduces to Eq. (1) in the simultaneous limit of  $n \rightarrow n_0$  and  $\alpha \rightarrow 0$ . We then set the nucleon distributions  $n_i(r)$  ( $i = n, p$ ) as

$$n_i(r) = \begin{cases} n_i^{\text{in}} \left[ 1 - \left( \frac{r}{R_i} \right)^{t_i} \right]^3, & r < R_i, \\ 0, & r \geq R_i, \end{cases} \quad (11)$$

and in the spirit of the Thomas-Fermi approximation minimize the total energy  $E$  with respect to  $R_i$ ,  $t_i$ , and  $n_i^{\text{in}}$  with the mass number  $A$ , the EOS parameters ( $n_0, w_0, S_0, K_0, L$ ) and the gradient coefficient  $F_0$  fixed. By calculating the charge number, mass excess, and root-mean-square charge radius from the minimizing values of  $R_i$ ,  $t_i$ , and  $n_i^{\text{in}}$  and fitting the results to the empirical values for stable nuclei ( $25 \leq A \leq 245$ ) on the smoothed beta stability line, we finally obtain  $n_0$ ,  $w_0$ ,  $S_0$ , and  $F_0$  for various sets of  $L$  and  $K_0$  ranging  $0 \text{ MeV} < L < 175 \text{ MeV}$  and  $180 \text{ MeV} \leq K_0 \leq 360 \text{ MeV}$ . We remark that as a result of this fitting, the parameters  $a_1$ - $b_2$  become functions of  $K_0$  and  $L$ , while we fix the remaining parameter  $b_3$ , which controls the EOS of matter for large neutron excess and high density, at  $1.58632 \text{ fm}^3$  throughout this fitting process.

The macroscopic nuclear models used here can describe gross nuclear properties such as masses and root-mean-square radii in a manner that is dependent on the EOS parameters,  $L$  and  $K_0$ . Notably, as in Ref. [2], these models predict that the root-mean-square matter radii increase appreciably with  $L$ , while being almost independent of  $K_0$ , and that the root-mean-square charge radii are almost independent of both  $L$  and  $K_0$ . However, there are some limitations in the present macroscopic approach. First, this approach works well in the range of  $\alpha \lesssim 0.3$  and  $A \gtrsim 50$ , where a macroscopic view of the system is relevant. Second, the nuclear surface is not satisfactory in the present Thomas-Fermi-type theory, which tends to underestimate the surface diffuseness and does not allow for the tails of the nucleon distributions. Lastly, no shell and pairing effects are included.

### III. GLAUBER MODEL

In the OLA of the Glauber model [8], the proton-nucleus scattering phase-shift function is simply de-

scribed by the proton density  $n_p(\mathbf{r})$  and the neutron density  $n_n(\mathbf{r})$  as follows:

$$e^{i\chi_{\text{OLA}}(\mathbf{b})} = \exp[i\chi_p(\mathbf{b}) + i\chi_n(\mathbf{b})], \quad (12)$$

where  $\chi_p$  ( $\chi_n$ ) is the phase shift due to protons (neutrons) inside the nucleus,

$$\begin{aligned} i\chi_p(\mathbf{b}) &= -\int dr n_p(\mathbf{r}) \Gamma_{pp}(\mathbf{b} - \mathbf{s}), \\ i\chi_n(\mathbf{b}) &= -\int dr n_n(\mathbf{r}) \Gamma_{pn}(\mathbf{b} - \mathbf{s}), \end{aligned} \quad (13)$$

with the impact parameter  $\mathbf{b}$  and the projection  $\mathbf{s}$  of the coordinate  $\mathbf{r}$  on a plane perpendicular to the incident proton momentum.

The profile function,  $\Gamma_{pN}$ , for  $pp$  and  $pn$  scatterings, is usually parametrized in the form:

$$\Gamma_{pN}(\mathbf{b}) = \frac{1 - i\alpha_{pN}}{4\pi\beta_{pN}} \sigma_{pN}^{\text{tot}} e^{-b^2/(2\beta_{pN})}, \quad (14)$$

where  $\alpha_{pN}$  is the ratio of the real to the imaginary part of the  $pp$  ( $pn$ ) scattering amplitude in the forward direction,  $\sigma_{pN}^{\text{tot}}$  is the  $pp$  ( $pn$ ) total cross section, and  $\beta_{pN}$  is the slope parameter of the  $pp$  ( $pn$ ) elastic scattering differential cross section. These parameters are tabulated for different incident energies in Ref. [9].

The total reaction cross section of the proton-nucleus collision is calculated from

$$\sigma_R = \int d\mathbf{b} \left(1 - |e^{i\chi_{\text{OLA}}(\mathbf{b})}|^2\right). \quad (15)$$

#### IV. EOS DEPENDENCE OF REACTION CROSS SECTIONS

In our calculation we have used a code based on the Monte Carlo integration for evaluations of the phase shift function, which can be applied to any arbitrary form of nucleon distributions. We have calculated the total reaction cross section for  $p$ - $^{63}\text{Cu}$ ,  $p$ - $^{80}\text{Ni}$ ,  $p$ - $^{112}\text{Sn}$ ,  $p$ - $^{124}\text{Sn}$ , and  $p$ - $^{208}\text{Pb}$  by substituting the distributions (11) determined as functions of  $L$  and  $K_0$  into  $n_{n,p}(\mathbf{r})$  in Eq. (13). For each system at each energy we have performed summation over 228 random points, which ensures sufficient accuracy.

Figure 1 shows the results for the selected isotopes at 800 MeV. As we pointed out in our previous paper [1] the dependence of the total reaction cross section on the EOS parameters is rather weak. By decreasing the energy to 300 MeV, we obtain the same conclusion as at 800 MeV; the results are shown in Fig. 2. Note that at such high energies the reaction cross section does not obey an empirical law obtained within a black sphere approximation [10], which suggests that the reaction cross section increases with the nuclear size and thus  $L$ . This is a feature to be discussed in more details below.

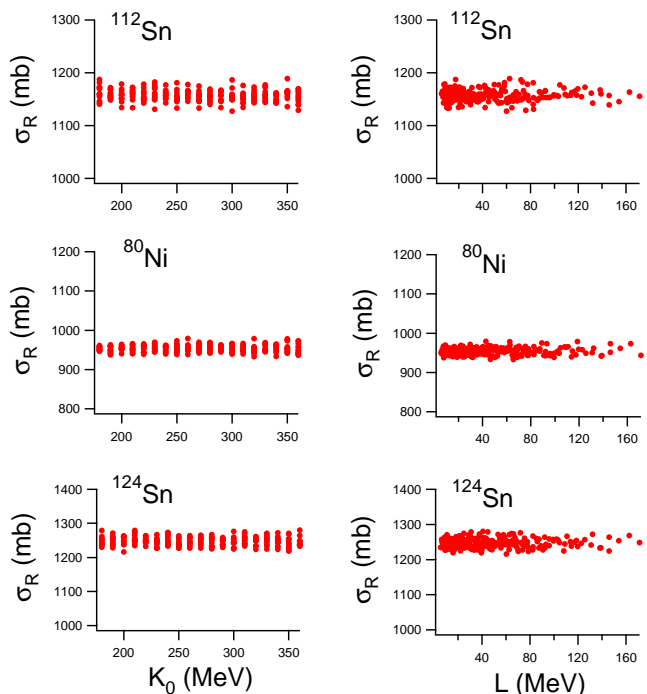


FIG. 1: (Color online) The total reaction cross sections calculated as a function of  $K_0$  and  $L$  for  $p$ - $^{112,124}\text{Sn}$  and  $p$ - $^{80}\text{Ni}$  at 800 MeV.

At 40 MeV the  $\sigma_{pn}^{\text{tot}}$  and  $\sigma_{pp}^{\text{tot}}$  are fairly large compared to those at 800 MeV, and  $\sigma_{pn}^{\text{tot}}$  is much larger than  $\sigma_{pp}^{\text{tot}}$ . Therefore we expect for neutron rich nuclei that the total reaction cross section depends sensitively on the neutron density distribution including the skin region.

Figure 3 shows our calculations of the reaction cross section as a function of  $L$  and  $K_0$ . We find, for neutron rich isotopes like  $^{80}\text{Ni}$  ( $Z/A = 0.35$ ), a strong dependence on the  $L$  value. The value of the total reaction cross section for  $(L, K_0) = (12.4, 350)$  in MeV is 1248 mb, while that for  $(L, K_0) = (171.3, 360)$  in MeV is 1346 mb. The difference between them is about 7%. If uncertainties of experimental data for the reaction cross section are less than about 3.5% and our calculations with simplified scattering theory and density distributions are satisfactory, we could determine the  $L$  value from comparison between the calculated and measured values.

For possible determination of  $L$ , therefore, it is important to examine how well the OLA of the Glauber model predicts the reaction cross section. Although this depends on the choice of density distributions, for simplicity, we here confine ourselves to rectangular nucleon distributions, for which one can calculate the reaction cross section analytically in the zero range limit ( $\beta_{pN} \rightarrow 0$ ).

Let us set the radius and density of the proton (neutron) distribution for a nucleus of given  $A$  and  $Z$  to be  $a_p$  ( $a_n$ ) and  $n_{p0} = 3Z/4\pi a_p^3$  [ $n_{n0} = 3(A-Z)/4\pi a_n^3$ ]. If  $a_p = a_n \equiv a$ , one can calculate the reaction cross section

(15) in the zero range limit as

$$\sigma_R = \pi a^2 \left[ 1 - \frac{2}{\xi^2} + \frac{2}{\xi} \left( 1 + \frac{1}{\xi} \right) e^{-\xi} \right], \quad (16)$$

where  $\xi = 2(\sigma_{pp}^{\text{tot}} n_{p0} + \sigma_{pn}^{\text{tot}} n_{n0})a$  is the effective optical depth. Note that in this case, the OLA of the Glauber model is strictly applicable when the effective optical depth is close to zero and the proton wave length is sufficiently short. In the limit of complete absorption ( $\xi \rightarrow \infty$ ), however, Eq. (16) reproduces the correct answer  $\pi a^2$ . One may thus expect that the OLA provides a fairly good prediction of the reaction cross section even for intermediate values of  $\xi$  as long as the incident energy is sufficiently high. Nevertheless, Eq. (16), if the exponential term in the right side works, is at odds with the power-law  $\sigma_{pN}^{\text{tot}}$  dependence of the reaction cross section that is empirically suggested [11]. Even if the exponential term is negligible, the energy dependence of the reaction cross section as deduced from Eq. (16) shows only a weak dependence on  $A$ , which is again at odds with the empirical behavior [12].

We now consider the case in which  $a_n$  and  $a_p$  are generally different from each other. In this case, as we shall see, the reaction cross section (15) in the zero range limit includes a term depending exponentially on the neutron skin thickness  $a_n - a_p$ . In fact, when one retains corrections to the black-disk limit ( $\sigma_{pN}^{\text{tot}} \rightarrow \infty$ ) by transparency of the skin region, the reaction cross section (15) in the

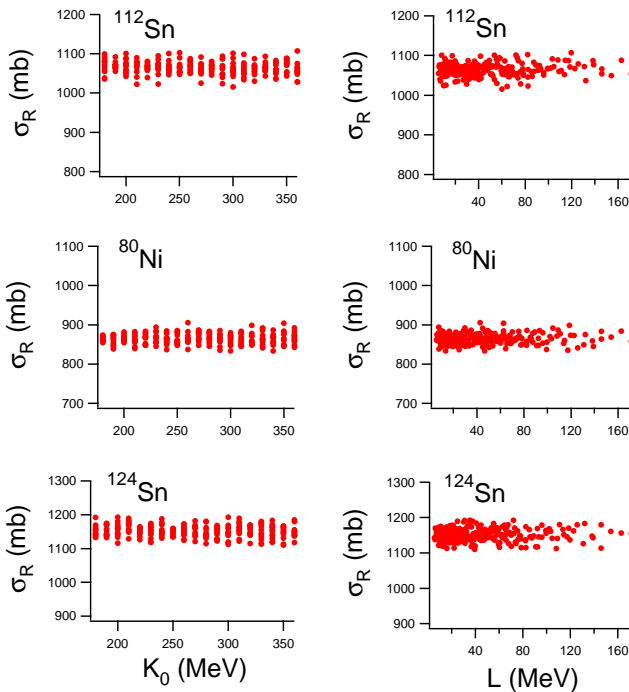


FIG. 2: (Color online) The total reaction cross sections calculated as a function of  $K_0$  and  $L$  for  $p$ - $^{112,124}\text{Sn}$  and  $p$ - $^{80}\text{Ni}$  at 300 MeV.

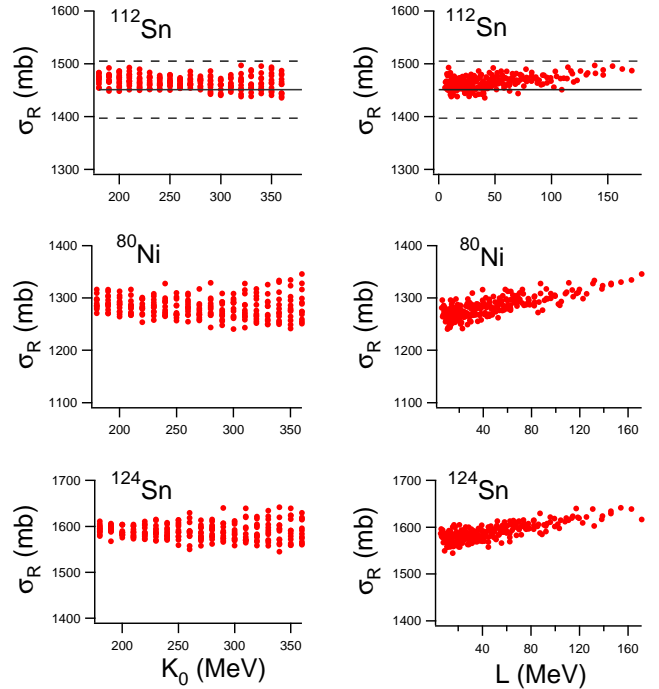


FIG. 3: (Color online) The total reaction cross sections calculated as a function of  $K_0$  and  $L$  for  $p$ - $^{112,124}\text{Sn}$  and  $p$ - $^{80}\text{Ni}$  at 40 MeV. The experimental values (solid lines: central values, dashed lines: upper and lower bounds) are taken from Ref. [14].

zero range limit has a form

$$\sigma_R \simeq \pi a_n^2 + 2\pi \left[ \frac{e^{-\zeta_n \sqrt{a_n^2 - a_p^2}}}{\zeta_n^2} \left( 1 + \zeta_n \sqrt{a_n^2 - a_p^2} \right) - \frac{1}{\zeta_n^2} \right], \quad (17)$$

where  $\zeta_n = 2\sigma_{pn}^{\text{tot}} n_{n0}$ .

It is instructive to note that Eq. (17) reduces to  $\pi a_n^2$  in the black-disk limit. For large but finite values of  $\zeta_n$ , the remaining term in the right side of Eq. (17) starts to play a role ahead of the corrections responsible for transparency of the inner region in which protons are present. Interestingly, this term is a decreasing function of  $a_n$  and in some cases acts to cancel an increase of the main term  $\pi a_n^2$  by an increment of  $a_n$ . As we shall see, this term is responsible for the  $L$  dependence of  $\sigma_R$  as shown in Figs. 1–3.

Let us now assume that the distribution (11) roughly corresponds to a rectangular one discussed above. Then, one can set the  $L$  and  $K_0$  dependence of  $a_n$  and  $a_p$  in such a way that  $a_n$  increases linearly with  $L$ , while any other dependence is negligibly weak (see Fig. 7 in Ref. [2]). For  $^{80}\text{Ni}$ , in particular, we set  $a_n$  and  $a_p$  as

$$a_n \approx 5.4 + 0.3 \left( \frac{L}{170 \text{ MeV}} \right) \text{ fm}, \quad (18)$$

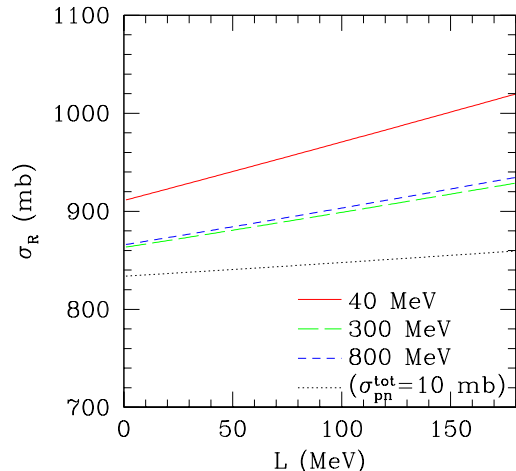


FIG. 4: (Color online) The total reaction cross sections calculated from Eq. (17) for  $^{80}\text{Ni}$  by using Eqs. (18) and (19) as  $a_n$  and  $a_p$ . The full, long-dashed, and short-dashed lines are the results obtained for  $\sigma_{pn}^{\text{tot}} = 220, 35, 38$  mb, which are relevant at incident energies of 40, 300, 800 MeV [13]. For comparison, we also plot by a dotted line the result obtained for  $\sigma_{pn}^{\text{tot}} = 10$  mb.

$$a_p \approx 5.1 \text{ fm}, \quad (19)$$

in reference to the root-mean-square neutron and proton radii calculated in Ref. [2]. Here we have taken into account a factor  $\sqrt{5/3}$ , which is the ratio of the half-density and root-mean-square radii for rectangular distributions. By using such a rough correspondence, we can understand the peculiar  $L$  dependence of  $\sigma_R$  obtained in the

OLA calculations.

In fact, as shown in Fig. 4, we find that Eq. (17) for various sets of  $\sigma_{pn}^{\text{tot}}$  gives a roughly linear dependence on  $L$ , while this dependence is suppressed for small values of  $\sigma_{pn}^{\text{tot}}$ . This is consistent with the tendency seen in Figs. 1-3, although higher order corrections to the black-disk limit have to be significant for small values of  $\zeta_n$  or, equivalently, small  $\sigma_{pn}^{\text{tot}}$ .

Figures 1-4 suggest that the magnitude of the reaction cross sections depends on the incident energy more remarkably in the OLA calculations than in Eq. (17). This is because in the OLA calculations we used the density distributions of form (11), which has a surface diffuseness and thus allow reactions to occur in an even farther region than the radius of the rectangular distributions.

In summary, we have discovered that the OLA of the Glauber theory exhibits a nonnegligible exponential dependence of the total proton-nucleus reaction cross sections on the neutron skin thickness at incident energies where  $\sigma_{pn}^{\text{tot}}$  is sufficiently small. It is, however, important to note that the validity of using the OLA of the Glauber theory in evaluating the total reaction cross sections in the energy range considered here is far from obvious. We also note that the Coulomb force ignored here has to play a role in distorting the proton trajectory at the lowest energy. For duly describing the energy and size dependence of the total reaction cross sections, therefore, alternative approaches based on empirical data for the total reaction cross sections such as those in Refs. [11, 15] might be useful.

## Acknowledgments

This work was supported in part by the Japan International Cultural Exchange Foundation (JICEF).

- 
- [1] K. Iida, K. Oyamatsu, and B. Abu-Ibrahim, Phys. Lett. B **576**, 273 (2003).  
 [2] K. Oyamatsu and K. Iida, Prog. Theor. Phys. **109**, 631 (2003).  
 [3] D.H. Youngblood, H.L. Clark, and Y.-W. Lui, Phys. Rev. Lett. **82**, 691 (1999).  
 [4] J.B. Natowitz, K. Hagel, Y. Ma, M. Murray, L. Qin, R. Wada, and J. Wang, Phys. Rev. Lett. **89**, 212701 (2002).  
 [5] M. Prakash, T.L. Ainsworth, and J.M. Lattimer, Phys. Rev. Lett. **61**, 2518 (1988).  
 [6] K. Oyamatsu and K. Iida, Phys. Rev. C **75**, 015801 (2007).  
 [7] K. Oyamatsu, Nucl. Phys. **A561**, 431 (1993).  
 [8] R.J. Glauber, in *Lectures in Theoretical Physics* (Interscience, New York, 1959), Vol. 1, p. 315.  
 [9] B. Abu-Ibrahim, W. Horiuchi, A. Kohama, and Y. Suzuki, Phys. Rev. C **77**, 034607 (2008).  
 [10] A. Kohama, K. Iida, and K. Oyamatsu, Phys. Rev. C **72**, 024602 (2005).  
 [11] A. Ingemarsson and M. Lantz, Phys. Rev. C **72**, 064615 (2005).  
 [12] A. Auce *et al.*, Phys. Rev. C **71**, 064606 (2005).  
 [13] From Particle Data Group via <http://pdg.lbl.gov/current/xsect/>.  
 [14] R.F. Carlson, At. Data Nucl. Data Tables **63**, 93 (1996).  
 [15] K. Iida, A. Kohama, and K. Oyamatsu, J. Phys. Soc. Jpn. **76**, 044201 (2007).